Inhibition of amyloid precursor protein secretases reduces recovery after spinal cord injury

Ahdeah Pajoohesh-Ganji[*,#], **Mark P. Burns**[&], **Sonali Pal-Ghosh**[*], **Gauri Tadvalkar**[*], **Nicole G. Hokenbury**, **Mary Ann Stepp**[*], and **Alan I. Faden**[+]

[*]The George Washington University, Washington DC

[&]Georgetown University, Washington DC

[+]University of Maryland, Baltimore

Abstract

Amyloid-β (Aβ) is produced through the enzymatic cleavage of amyloid precursor protein (APP) by β (Bace1) and γ -secretases. The accumulation and aggregation of Aβ as amyloid plaques is the hallmark pathology of Alzheimer's disease and has been found in other neurological disorders, such as traumatic brain injury and multiple sclerosis. Although the role of Aβ after injury is not well understood, several studies have reported a negative correlation between Aβ formation and functional outcome. In this study we show that levels of APP, the enzymes cleaving APP (Bace1 and γ-secretase), and Aβ are significantly increased from 1 to 3 days after impact spinal cord injury (SCI) in mice. To determine the role of Aβ after SCI, we reduced or inhibited Aβ *in vivo* through pharmacological (using DAPT) or genetic (*Bace1* knockout mice) approaches. We found that these interventions significantly impaired functional recovery as evaluated by white matter sparing and behavioral testing. These data are consistent

Keywords

Spinal cord injury; Amyloid precursor protein; γ-secretase; Bace1; amyloid-β

Introduction

Amyloid-β (Aβ) is the product of the sequential cleavage of amyloid precursor protein (APP) by β- (BACE-1) and γ- secretases (Hu et al, 2006; Selkoe, 2004). Considerable data support a pathophysiological role for Aβ in Alzheimer's disease. Increases in APP, Bace-1, γ- secretase, and Aβ have also been observed with the onset of several other neurological

Author Disclosure Statement: No competing financial interests exist.

disorders. Amyotrophic lateral sclerosis (ALS) onset is accompanied by an increase in APP, and elevated levels of both APP and Aβ have been observed in motor neurons and their surrounding glial cells in the spinal cord of ALS mouse models (Bryson et al., 2012). Patients with multiple sclerosis (MS) show APP up-regulation in both acute and chronic lesions (Ikonomovic et al. 2004) and APP expression has been suggested as a biomarker for disease progression (Gehrmann et al., 1995). Aβ has also been implicated in microglial activation and associated neuroinflammation (Matsuoka et al., 2001; Wyss-Coray and Mucke, 2002).

In postmortem studies, Aβ deposits have been observed following traumatic brain injury (TBI) (Roberts et al., 1991; Roberts et al., 1994). Studies on excised surgery tissues show that Aβ accumulation is occurring in as little as two hours (Ikonomovic et al., 2004). The accumulation of Aβ also occurs in animal models of TBI (Iwata et al., 2002; Uryu et al., 2002). APP, BACE1, and PS1 are increased in the areas of axonal injury as early as 2h after TBI (Chen et al., 2004; Uryu et al., 2007). Elevated levels of Aβ positively correlate with increases in β- and γ- secretases (Blasko et al., 2004). We recently demonstrated that inhibiting the activity of APP secretases and Aβ is protective in a mouse model of TBI (Loane et al., 2009), suggesting that Aβ may be contributing to secondary injury cascades after TBI. APP is also increased after spinal cord injury (SCI), in both humans and rodents (Ahlgren et al., 1996; Choo et al., 2008; Cornish et al., 2000; Li et al., 1995). A recent study in rats shows that the increase in APP and PS1 is accompanied by an increase in Aβ peptide levels as early as 1 day after spinal cord hemisection. This increase appears to occur within the axons in the white matter at the site of injury (Kobayashi et al., 2010). However, the injury-induced changes in APP secretases are not limited to neurons. After brain trauma, an increase in Bace 1 and PS1 was reported in astrocytes (Blasko et al, 2004) and in both astrocytes and microglial cells, respectively (Nadler et al., 2008).

Although Aβ is implicated as a pathobiological factor in several neurological disorders, recent studies suggest that it may also have a protective role. Using a mouse model of MS — experimental autoimmune encephalomyelitis (EAE) — investigators demonstrated that Aβ pep tide injections decreased paralysis and brain inflammation by suppressing activated lymphocytes (Grant et al., 2012). *Bace1* knockout (*Bace1* KO) mice, which do not produce Aβ, (Cai et al., 2001; Lu et al., 2000) show increased motor and cognitive deficits after TBI in the KO mice as compared to wild type controls (Mannix et al., 2011). To address the role of Aβ after SCI, we used a mouse spinal contusion model to examine effects of injury on APP, PS1, Bace1, and Aβ production. We also prevented Aβ formation after SCI using the γ-secretase inhibitor DAPT (N-[(3, 5-Difluorophenyl) acetyl]-L-alanyl-2-phenyl]glycine-l,l-dimethylethyl ester) or *Bace1* KO mice.

Results

SCI increases APP, PS1, and Bace-1

To study the expression of APP and PS1 before and after SCI, mice were sacrificed as sham or at 1, 3 and 7 days after moderate-severe injury (n=4/group). Figure 1A shows sections from sham and 1, 3, and 7 day post injury (DPI) at the epicenter. Regions identified by asterisk and arrowhead are magnified in Figure 1B. In sham, APP and PS1 are co-localized

in the motor neurons in gray matter and the glial cells present in both white and gray matter. PS1 and APP increase at 1 and 3 days after injury, especially in the white matter, and return toward baseline by 7 DPI. APP and PS1 co-localize more after SCI injury as evident by the increased overlap of red and green in the merged images as compared to sham. Figure 1C is a representative high resolution confocal image (taken from the area indicated in the thumbnail image by arrowhead) showing that some of the Iba 1+ microglia express PS1 at 1DPI.

Sections 1mm and 2mm rostral and caudal from the epicenter were evaluated from sham and injured mice (n=3/group) at 1, 3 and 7 days after injury using PS1. Figure 2A shows a representative image and Figure 2B summarizes the quantitative data. The thumbnail image represents the negative control for PS1. There is a significant increase (p-value < 0.02), in PS1 protein 1 and 3 days after injury at the epicenter, as well as 1 mm rostral (p-value < 0.001) and caudal (p-value < 0.005) from the injury site. At 2 mm rostral (p-value < 0.0001) and caudal (p-value < 0.04) to the epicenter, a significant increase is only observed at 1 day after injury. The increase of PS1 in injured tissue compared to sham was confirmed using Western blots (Figure 2C); PS1 protein levels are significantly increased (p-value < 0.05) at 1 and 3 days after injury. Figure 2D indicates that Bace1 protein levels are also significantly increased (p-value < 0.05) at 1 DPI.

SCI acutely increases A/β accumulation

To determine whether the increase in APP and its secretases is functionally relevant, mice (n=4/group) were injured and sacrificed at 1, 3, 7, 14, 21, and 28 days after SCI. $A\beta_{40}$ELISA was performed on the diethylamine (DEA) extraction and Aβ was measured as fmol/mg protein (Figure 3). There are no significant differences in Aβ levels between naïve mice and sham mice euthanized 3 days post-surgery (n=4/group) indicating that laminectomy alone did not cause $A\beta_{40}$ up-regulation. Aβ is significantly increased (p-value < 0.01) at 1 and 3 days after SCI compared to sham or naïve samples. The increase in Aβ is concurrent with the increase in APP and its secretases.

DAPT significantly reduces A/β accumulation after SCI

In order to confirm that the γ-secretase inhibitor DAPT can reduce the production of Aβ after SCI, C57/B16 spinal cord injured and sham mice (n=4/group) were administered either DAPT or vehicle as described in the Materials and Methods. Similar to our earlier experiment, SCI caused a significant increase in Aβ levels compared to sham injured mice. DAPT significantly (p-value < 0.01) attenuated the SCI-induced increase in Aβ at 3d post-injury by 30% (Figure 4).

DAPT administration reduces functional recovery after SCI in mice as measured by BMS and BLG

To investigate the effects of DAPT on functional recovery, C57/B16 injured mice (n=12/group) were administered either DAPT (30mg/kg) or vehicle orally twice a day starting 15 minutes after injury for 10 days. Functional recovery was evaluated using BMS (Basso mouse scale, range of 0–9, 9 being a normal mouse) 1 day after injury and weekly thereafter (Figure 5A). Furthermore, BLG (Basso mouse scale/Ladder climb/Grid walk) score (range

of 0–27, 27 being a normal mouse) was evaluated 7 days after injury on a weekly basis until 28 days after SCI (Figure 5B), at which time mice were sacrificed and spinal cords removed and processed to assess white matter sparing. BLG scoring method employs and combines three tests (BMS, modified ladder climb and grid walk) and is shown to be a more sensitive functional test than BMS alone (Pajoohesh-Ganji et al., 2010). BMS indicates that vehicle-treated mice have a score of 4.5 +/− 0.2 at 28 days post-injury representing achievement of frequent or consistent plantar stepping. DAPT-treated mice, on the other hand, have a score of 3.9 +/− 0.2 at day 28, a significant decrease (p-value < 0.04) over vehicle treated mice. In the vehicle group, only 2 out of 12 mice show a score less than 4, which indicates lack of plantar stepping, whereas half (6 of 12) of the mice in the DAPT-treated group are not able to achieve plantar stepping and receive a score less than 4.

Using BLG score, significant differences (p-value < 0.04) between vehicle- and DAPT-treated mice are observed as early as 7 days after injury and persist until 28 days post-injury (p-value < 0.02). While vehicle-treated mice have a score of 12.1+/− 1.9 at day 28, DAPT-treated mice are significantly worse at day 28, only achieving a score of 6.4 +/− 1.1 (p-value < 0.04 compared to vehicle-treated mice). Quantitation of white matter sparing shows that vehicle-treated mice have a significantly greater (p-value = 0.04) amount of white matter spared than DAPT-treated mice 28 DPI (Figure 5C). Furthermore, representative images with Eriochrome cyanine R staining at the epicenter show the differences between the vehicle and DAPT treated injured mice (Figure 5D).

Bace1 knockout mice have impaired functional recovery after SCI as measured by BMS and BLG

To further investigate the role of the APP secretases after SCI, *Bace1* KO (n=7) and WT mice (n=6) were injured, as previously described. Naive mice (n=4) were evaluated and Eriochrome staining from WT and *Bace1* KO are presented in Figure 6A. Functional recovery in injured mice was evaluated using BMS and BLG scoring and white matter sparing was assessed. Utilizing BMS, WT mice reach a score of 4.5 +/− 0.4 at 28 DPI, representing frequent or consistent plantar stepping. *Bace1* KO mice, on the other hand, have a score of 3.4 +/− 0.1 at day 28, a significant decrease (p-value < 0.01) as compared to WT mice (Figure 6B). In WT, only 1 out of 6 mice have a score less than 4, whereas 6 out of 7 *Bace1* KO mice are not able to achieve plantar stepping and receive a score less than 4, at 28 DPI. Using BMS, a significant difference in functional recovery is observed at days 14 (p-value < 0.004) and 21 (p-value < 0.005). All naive mice had a score of 9 at all the time points.

Using BLG score, significant differences between WT and *Bace1* KO mice are also observed at 14 DPI (p-value < 0.04) and these differences persistently increase to 28 DPI (p-value < 0.01). WT mice achieve a score of 13.2 +/− 2.8 whereas the *Bace1* KO mice have a score of 5.7 +/− 0.8 at day 28, a significant decrease (p-value <0.01) as compared to WT mice (Figure 6C). All naive mice had a score of 27 at all the time points. Quantitation of white matter sparing show that WT mice have a significantly greater (p-value = 0.03) amount of white matter spared than *Bace1* KO mice 28 DPI (Figure 6D). Representative images using Eriochrome cyanine R staining show the differences between the WT and

Bace1 KO mice after injury (Figure 6E). However, gray matter quantitation showed no differences between WT and *Bace1* KO mice 28 DPI (p-value = 0.22). Taken together, our data indicate that reducing Aβ formation after SCI decreases the functional recovery.

Bace1 knockout mice have less microglia after SCI

To investigate whether the decrease in Aβ has an effect on microglial number, sections from vehicle, DAPT treated, *Bace1* KO, and WT mice were stained with a microglial marker, Iba1. Confocal images were taken from the epicenter, 200, and 400 μm rostral and caudal and analyzed using image J. As shown in the graph and representative images, there are no differences in the number of microglia in DAPT-treated as compared to vehicle-treated mice (Figure 7A). However, microglial number is significantly (p value = 0.002) lower in the *Bace1* KO as compared to WT mice (Figure 7B).

Discussion

SCI causes delayed biochemical changes, known as secondary injury, which leads to additional tissue damage and cell death (Panter and Faden, 1992). Secondary injury mechanisms include inflammation and reactive astrogliosis and microglial activation, which are involved in scar formation and impaired regeneration (Lu et al., 2000). Among the biochemical changes are increases in APP, its secretases, and Aβ shown in this and other studies of human and rat tissues (Ahlgren et al., 1996; Choo et al., 2008; Cornish et al., 2000; Kobayashi et al., 2010; Li et al., 1995).

Aβ has been shown to activate microglia and inflammatory pathways and cause neuronal cell death (Matsuoka et al., 2001; Wyss-Coray and Mucke, 2002). Microglial activation is characterized by transition of quiescent microglia from a resting, ramified to an ameboid, 'macrophage-like' phenotype capable of both phagocytosis and proliferation (Raivich et al., 1999). Depending on the signals provided by the microenvironment present at the injury site, microglia can either differentiate into "classically activated" M1 microglia, which are neurotoxic and produce high levels of pro-inflammatory cytokines, or "alternatively activated" M2 microglia that promote plasticity and axonal outgrowth and inhibit inflammation (Kigerl et al., 2009; Pajoohesh-Ganji and Byrnes, 2011). These phenotypes elucidate how microglial activation promote Aβ and myelin debris clearance (Farah et al., 2011; Mandrekar et al., 2009) while triggering a pro-inflammatory response (Hickman et al., 2008) and why microglial activation is referred to as a "double-edged sword" (Mannix and Whalen, 2012; Wyss-Coray and Mucke, 2002).

As Aβ is a known key mediator of microglial activation and a neurotoxic pep tide, the main question in this report is whether Aβ enhances or impedes recovery after SCI in mice. Our data indicate that APP, Bace1, γ-secretase, and Aβ are significantly increased between 1 and 3 days after injury. These results are consistent with prior literature in SCI. We also show for the first time that reducing or inhibiting Aβ formation through pharmacological (using DAPT) and genetic (*Bace1* KO mice) methods exacerbates the functional outcome after SCI as evaluated by level of white matter spared and behavioral testing.

Aβ is also increased after brain trauma in mice (Loane et al., 2009). In contrast to the present findings, inhibiting the APP secretases after TBI led to improved functional recovery. The differences seen between this study and the Loane study could be due to the fact that DAPT treatment was maintained for 21 days in the TBI study, as compared to 10 days for our SCI studies. The reason we did not continue DAPT treatment longer is because our time course experiments clearly showed that PS1, Bace1 and Aβ had all returned to baseline levels by 7 days post-SCI. Moreover, our studies were performed on younger mice (5–6 month old) than the mice in Loane study (11–12 month old). Conversely, another study found that *Bace1* KO mice (2–3 month old) had worse functional recovery after TBI (Manix et al., 2011). Based on these studies, age seems to be a factor in the outcome after trauma. Furthermore, our findings also appear consistent with the observation that systemic injection of Aβ pep tides decreases paralysis and brain inflammation in a mouse model of EAE (Grant et al., 2012).

As it is widely considered that secondary injury processes are similar between SCI and TBI, such differences may suggest a more fundamental distinction across these trauma models with regards to the roles of APP processing or down-stream secretase targets. However, acute inflammatory responses are greater in spinal cord than in the brain, possibly reflecting more BBB breakdown after SCI that leads to higher number of microglia, neutrophils, and macrophages recruited to the site of injury (Batchelor et al., 2008; Carlson et al., 1998; Schnell et al., 1999a; Schnell et al., 1999b). There was no difference between microglial numbers in vehicle- vs. DAPT-treated mice, which indicates that DAPT did not fully inhibit Aβ production, as evident in Figure 4. However, *Bace1* KO mice do not produce Aβ. Our data show a reduced number of microglia in the *Bace1* KO mice, consistent with the ability of Aβ to induce microglial activation. Perhaps surprisingly, this reduction in microglial number was associated with worse functional recovery. This may be due to the fact that inhibiting Aβ may potentially decrease M2 microglial activation, which may sub-serve more protective roles. Further studies will be required to elucidate the effects of Aβ in modulating the relative activation patterns of M1 versus M2 microglial pathways after SCI.

Alternatively, it must be recognized that in addition to APP, γ-secretase and Bace1 cleave multiple other proteins, including Notch 1 and neuregulin 1 type III (NRG1) respectively. Inhibiting cleavage of Notch 1 and NRG 1 in DAPT and *Bace1* KO mice may serve to modify signaling pathways unrelated to APP processing. Upon ligand binding, Notch intracellular domain (NICD) is produced by the cleavage of Notch 1 via γ-secretase and a metalloproteinase. NICD translocates to the nucleus and triggers the transcription of target genes, which depending on the ligand may suppress or promote proliferation and differentiation of oligodendrocyte precursor cells (Brosnan and John, 2009; D'Souza et al., 2008; De Strooper and Konig, 1999; Gaiano et al., 2000; Tanigaki et al., 2001). Furthermore, NRG1 mediates myelin sheet thickness and determines the caliber of axons (Velanac et al., 2012). *Bace1* KO mice have severe hypomyelination of their peripheral and central nervous system (Hu et al., 2006; Hu et al., 2008), increased lethality rates during the early postnatal developmental period, and hyperactivity (Dominguez et al., 2005). Processing of NRG1 has been shown to be impaired but not abolished in *Bace1* KO mice (Hu et al., 2006; Hu et al., 2013; Velanac et al., 2012). Therefore, the reduced white matter

sparing observed in the *Bace1* KO mice after SCI may in part reflect the reduced NRG1 signaling or less myelin in the *Bace1* KO mice prior to injury.

Materials and Methods

Mice

2–3 month old C57B1/6 mice were purchased from Taconic. For the *Bace1* KO study, we decided to use older mice to compare with our previous study performed in TBI (Loane et al., 2009). However to decrease the mortality rate due to age, we purchased 5–6 month old *Bace1* KO mice and aged matched controls from Jackson Laboratories. All experiments fully complied with the principles set forth in the "Guide for the Care and Use of Laboratory Animals and were approved by the Georgetown university and The George Washington University Animal Care and Use Committees.

Spinal Cord Injury

Mice were anesthetized using isoflurane (Baxter, Deerfield, IL; E-Z system Bio Vac chamber). The mouse was placed in the chamber and the isofurane vaporizer was originally set at 5%. Once the mouse was fully anesthetized, it was removed from the chamber and placed on a nose cone with a maintenance dose at 2%. A laminectomy was performed at the T-9 level for sham and all injured animals. The spinal cord was stabilized using mouse transverse clamps (Stoelting, Wood Dale, IL). A 1.85 g weight was dropped from 20 mm onto an impounder positioned on the exposed spinal cord, as previously described (Pajoohesh-Ganji et al., 2010). Sham animals (n=4) received a laminectomy without contusion injury and naïve mice (n=4) served as additional controls in ELISA studies. Sham mice were obtained at 3 days (n=4/group) after laminectomy. Bladder expression on injured animals was performed twice daily until autonomic bladder function returned. For ELISA, Western blot analysis, and immunofluorescence staining mice were sacrificed at various time points after SCI: 1,3,7, 14, 21, and 28 days (n=4). Behavioral studies were performed 1 day after injury and on weekly basis thereafter; mice were sacrificed at 28 days after injury (n=12).

DAPT administration

DAPT (Calbiochem), a γ-secretase inhibitor, was made in 5% ethanol in corn oil and administered orally at a volume of 5ml/kg with a final dose of 30mg/kg as previously described (Loane et al., 2009). Vehicle was 5% ethanol in corn oil and was administered as 5ml/kg. Each mouse received the initial dose 15 minutes after SCI or sham injury and twice daily for either 3 days (ELISA studies) or 10 days (behavioral studies) after SCI. Animals were monitored daily for signs of distress and gastrointestinal discomfort. Although we did not specifically measure body weight or food consumption, there were no apparent differences observed between DAPT- and vehicle-treated mice. Furthermore, others have shown DAPT does not significantly change animal body weight (Saeidi et al., 2013). Mice were euthanized 12 hours following the final dose of DAPT in the ELISA studies.

A/3ELISA and Western blotting

Proteins for ELISA and Western blots were sequentially extracted, as previously described (Loane et al., 2009), from a total of 5mm of spinal cord (2.5mm rostral and 2.5mm caudal to the injury site) in diethylamine (DEA) and RIPA buffer. A commercially available kit from Wako Chemicals (Richmond, VA) was used to detect endogenous soluble mouse $A\beta_{x-40}$, as per manufacturer's instructions from the DEA extractions. Western blots were performed as previously described (Byrnes et al., 2007). DEA extracts were used for Bace1 (Millipore, Cat # MAB5308, 1:500) and the RIPA extracts were used for PS1 (Millipore, Cat # MAB5232, 1:1000). Pixel intensity for each sample and its corresponding actin (Millipore, #MAB1501R at 1:2000) was measured on three different blots using Image J software. To quantify the results, samples were normalized to actin and a graph was made using GraphPad Prism Program, Version 4 for Windows (GraphPad Software, Inc. San Diego, CA).

Behavioral testing

Mice were tested for hindlimb functional deficits after SCI in a blinded fashion. Hindlimb locomotor recovery was assessed in an open field using the BMS (Basso Mouse scale) (Basso et al., 2006) and BLG (Basso mouse scale/Ladder climb/Grid walk) (Pajoohesh-Ganji et al., 2010) scoring methods at 1, 7, 14, 21, and 28 DPI. Mice were excluded from the studies if the BMS was greater than 1 on day 1 after SCI. In the *Bace1* KO study, n=4 in the wild type and n=3 in the KO group had to be excluded from the study because they had a BMS of 2 or greater at 1 day after SCI.

Stereological quantitation of white matter sparing

Animals were anesthetized (100 mg/Kg sodium pentobarbital, I.P.) and intracardially perfused with 50 ml of 0.9% heparinized saline followed by 50 ml of 10% buffered formalin at different time points after injury (1, 3, 7, 14, 21, 28 days and sham mice). A 0.5 cm section of the spinal cord centered at the lesion epicenter was dissected, post-fixed in 10% buffered formalin overnight, and cryoprotected in 10, 20, and 30% sucrose overnight. Sections were embedded in OCT compound (Andwin Scientific Tissue-Tek) and cut at 20μm onto SuperFrost slides (Fisher, Cat#12-550-15). Quantitative assessment of white matter sparing was performed using the Cavalieri method of unbiased stereology. Every 40th section of the 0.5 cm spinal cord block, with a random starting section, was processed with a standard Eriochrome cyanine R staining protocol for histological analysis. Volume estimations were obtained from at least 10 randomly selected sections spanning 0.5 cm centered around the lesion site, as previously described (Donnelly et al., 2009; Pajoohesh-Ganji et al., 2010).

Immunostaining

Sections from various time points were stained against APP (Abeam, #ab 12270, at 1:100), PS1 (Millipore, #MAB5232 at 1:200), andlbal (Abeam, #ab5076, at 1:200) followed by appropriate secondary antibodies. To ensure accurate and specific staining, negative controls were used. Immunofluorescence was detected using confocal microscopy or an AxioPlan Zeiss Microscopy system (Carl Zeiss, Inc., Thornwood, NY). Tile and individual images

were taken using a 20× objective. The images were first optimized for the 1 day time point, which has the most PS1, followed by the other time points without changing the intensity. Immunolabeling was quantified as previously described (Pajoohesh-Ganji et al., 2012).

Statistical analyses

Quantitative data are presented as mean +/− standard error of the mean. All data were analyzed using Student's t-test or repeated measures ANOVA. All statistical tests were performed using the GraphPad Prism Program, Version 4 for Windows (GraphPad Software, Inc. San Diego, CA). A p value < 0.05 was considered statistically significant.

Conclusion

In conclusion, we have demonstrated that APP and the APP secretase proteins, Bace1 and PS1, accumulate acutely in an experimental model of SCI. This is a functional accumulation, which leads to the production of Aβ peptide at the injury site. We further demonstrated that inhibiting Aβ production by targeting the APP secretases results in greater white matter loss and impaired functional recovery after SCI. Further *in vivo* studies are required to better clarify the relative roles of APP processing and Aβ generation, Notch signaling, and NRG1 signaling in the responses of the brain and spinal cord to traumatic injuries.

Acknowledgments

Abbreviations

|	
Aβ	amyloid-β
ALS	amyotrophic lateral sclerosis
APP	amyloid precursor protein
BLG	Basso mouse scale/Ladder climb/Grid walk
BMS	Basso mouse scale
DAPT	N-[(3, 5-Difluorophenyl)acetyl]-L-alanyl-2-phenyl]glycine-l, l-dimethylethyl ester
DEA	diethylamine
DPI	days post-injury
EAE	experimental autoimmune encephalomyelitis
MS	multiple sclerosis
SCI	spinal cord injury

| **TBI** | traumatic brain injury |

References

Ahlgren S, et al. Accumulation of beta-amyloid precursor protein and ubiquitin in axons after spinal cord trauma in humans: immunohistochemical observations on autopsy material. Acta Neuropathol. 1996; 92:49–55. [PubMed: 8811125]

Basso DM, et al. Basso Mouse Scale for locomotion detects differences in recovery after spinal cord injury in five common mouse strains. J Neurotrauma. 2006; 23:635–659. [PubMed: 16689667]

Batchelor PE, et al. Comparison of inflammation in the brain and spinal cord following mechanical injury. J Neurotrauma. 2008; 25:1217–1225. [PubMed: 18986223]

Blasko I, et al. Experimental traumatic brain injury in rats stimulates the expression, production and activity of Alzheimer's disease beta-secretase (BACE-1). J Neural Transm. 2004; 111:523–536. [PubMed: 15057522]

Brosnan CF, John GR. Revisiting Notch in remyelination of multiple sclerosis lesions. J Clin Invest. 2009; 119:10–13. [PubMed: 19104146]

Bryson JB, et al. Amyloid precursor protein (APP) contributes to pathology in the SOD1(G93A) mouse model of amyotrophic lateral sclerosis. Hum Mol Genet. 2012; 21:3871–3882. [PubMed: 22678056]

Byrnes KR, et al. Cell cycle activation contributes to post-mitotic cell death and secondary damage after spinal cord injury. Brain. 2007; 130:2977–2992. [PubMed: 17690131]

Cai H, et al. BACE1 is the major beta-secretase for generation of Abeta peptides by neurons. Nat Neurosci. 2001; 4:233–234. [PubMed: 11224536]

Carlson SL, et al. Acute inflammatory response in spinal cord following impact injury. Exp Neurol. 1998; 151:77–88. [PubMed: 9582256]

Chen XH, et al. Long-term accumulation of amyloid-beta, beta-secretase, presenilin-1, and caspase-3 in damaged axons following brain trauma. Am J Pathol. 2004; 165:357–371. [PubMed: 15277212]

Choo AM, et al. Secondary pathology following contusion, dislocation, and distraction spinal cord injuries. Exp Neurol. 2008; 212:490–506. [PubMed: 18561916]

Cornish R, et al. Topography and severity of axonal injury in human spinal cord trauma using amyloid precursor protein as a marker of axonal injury. Spine (Phila Pa 1976). 2000; 25:1227–1233. [PubMed: 10806498]

D'Souza B, et al. The many facets of Notch ligands. Oncogene. 2008; 27:5148–5167. [PubMed: 18758484]

De Strooper B, Konig G. Alzheimer's disease. A firm base for drug development. Nature. 1999; 402:471–472. [PubMed: 10591201]

Dominguez D, et al. Phenotypic and biochemical analyses of BACE1- and BACE2-deficient mice. J Biol Chem. 2005; 280:30797–30806. [PubMed: 15987683]

Donnelly DJ, et al. An efficient and reproducible method for quantifying macrophages in different experimental models of central nervous system pathology. J Neurosci Methods. 2009; 181:36–44. [PubMed: 19393692]

Farah MH, et al. Reduced BACE1 activity enhances clearance of myelin debris and regeneration of axons in the injured peripheral nervous system. J Neurosci. 2011; 31:5744–5754. [PubMed: 21490216]

Gaiano N, et al. Radial glial identity is promoted by Notchl signaling in the murine forebrain. Neuron. 2000; 26:395–404. [PubMed: 10839358]

Gehrmann J, et al. Amyloid precursor protein (APP) expression in multiple sclerosis lesions. Glia. 1995; 15:141–151. [PubMed: 8567065]

Grant JL, et al. Reversal of paralysis and reduced inflammation from peripheral administration of beta-amyloid in TH1 and TH17 versions of experimental autoimmune encephalomyelitis. Sci TransI Med. 2012; 4:145ra105.

Hickman SE, et al. Microglial dysfunction and defective beta-amyloid clearance pathways in aging Alzheimer's disease mice. J Neurosci. 2008; 28:8354–8360. [PubMed: 18701698]

Hu X, et al. Bace1 modulates myelination in the central and peripheral nervous system. Nat Neurosci. 2006; 9:1520–1525. [PubMed: 17099708]

Hu X, et al. Genetic deletion of BACE1 in mice affects remyelination of sciatic nerves. FASEB J. 2008; 22:2970–2980. [PubMed: 18413858]

Hu X, et al. Reversing hypomyelination in Bace1-null mice with Akt-DD overexpression. FASEB J. 2013; 27:1868–1873. [PubMed: 23335052]

Ikonomovic MD, et al. Alzheimer's pathology in human temporal cortex surgically excised after severe brain injury. Exp Neurol. 2004; 190:192–203. [PubMed: 15473992]

Iwata A, et al. Long-term accumulation of amyloid-beta in axons following brain trauma without persistent upregulation of amyloid precursor protein genes. J Neuropathol Exp Neurol. 2002; 61:1056–1068. [PubMed: 12484568]

Kigerl KA, et al. Identification of two distinct macrophage subsets with divergent effects causing either neurotoxicity or regeneration in the injured mouse spinal cord. J Neurosci. 2009; 29:13435–13444. [PubMed: 19864556]

Kobayashi S, et al. Temporal-spatial expression of presenilin 1 and the production of amyloid-beta after acute spinal cord injury in adult rat. Neurochem Int. 2010; 56:387–393. [PubMed: 19932144]

Li GL, et al. Changes of beta-amyloid precursor protein after compression trauma to the spinal cord: an experimental study in the rat using immunohistochemistry. J Neurotrauma. 1995; 12:269–277. [PubMed: 7473801]

Loane DJ, et al. Amyloid precursor protein secretases as therapeutic targets for traumatic brain injury. Nat Med. 2009; 15:377–379. [PubMed: 19287391]

Lu J, Ashwell KW, Waite P. Advances in secondary spinal cord injury: role of apoptosis. Spine (Phila Pa 1976). 2000; 25:1859–1866. [PubMed: 10888960]

Mandrekar S, et al. Microglia mediate the clearance of soluble Abeta through fluid phase macropinocytosis. J Neurosci. 2009; 29:4252–4262. [PubMed: 19339619]

Mannix RC, et al. Detrimental effect of genetic inhibition of B-site APP-cleaving enzyme 1 on functional outcome after controlled cortical impact in young adult mice. J Neurotrauma. 2011; 28:1855–1861. [PubMed: 21639727]

Mannix RC, Whalen MJ. Traumatic brain injury, microglia, and Beta amyloid. Int J Alzheimers Dis. 2012; 2012:608732. [PubMed: 22666622]

Matsuoka Y, et al. Inflammatory responses to amyloidosis in a transgenic mouse model of Alzheimer's disease. Am J Pathol. 2001; 158:1345–1354. [PubMed: 11290552]

Nadler Y, et al. Increased expression of the gamma-secretase components presenilin-1 and nicastrin in activated astrocytes and microglia following traumatic brain injury. Glia. 2008; 56:552–567. [PubMed: 18240300]

Pajoohesh-Ganji A, et al. A combined scoring method to assess behavioral recovery after mouse spinal cord injury. Neurosci Res. 2010; 67:117–125. [PubMed: 20188770]

Pajoohesh-Ganji A, Byrnes KR. Novel neuroinflammatory targets in the chronically injured spinal cord. Neurotherapeutics. 2011; 8:195–205. [PubMed: 21394541]

Pajoohesh-Ganji A, et al. Characterization of inflammatory gene expression and galectin-3 function after spinal cord injury in mice. Brain Res. 2012; 1475:96–105. [PubMed: 22884909]

Panter SS, Faden AI. Pretreatment with NMDA antagonists limits release of excitatory amino acids following traumatic brain injury. Neurosci Lett. 1992; 136:165–168. [PubMed: 1353624]

Raivich G, et al. Neuroglial activation repertoire in the injured brain: graded response, molecular mechanisms and cues to physiological function. Brain Res Brain Res Rev. 1999; 30:77–105. [PubMed: 10407127]

Roberts GW, et al. beta A4 amyloid protein deposition in brain after head trauma. Lancet. 1991; 338:1422–1423. [PubMed: 1683421]

Roberts GW, et al. Beta amyloid protein deposition in the brain after severe head injury: implications for the pathogenesis of Alzheimer's disease. J Neurol Neurosurg Psychiatry. 1994; 57:419–425. [PubMed: 8163989]

Saeidi H, et al. Effects of DAPT on serum Vascular Endothelial Growth Factor and its soluble receptor in obese BALB/C mice. J of Isfahan Medical School. 2013; 30:1942–1948.

Schnell L, et al. Acute inflammatory responses to mechanical lesions in the CNS: differences between brain and spinal cord. Eur J Neurosci. 1999a; 11:3648–3658. [PubMed: 10564372]

Schnell L, et al. Cytokine-induced acute inflammation in the brain and spinal cord. J Neuropathol Exp Neurol. 1999b; 58:245–254. [PubMed: 10197816]

Selkoe DJ. Alzheimer disease: mechanistic understanding predicts novel therapies. Ann Intern Med. 2004; 140:627–638. [PubMed: 15096334]

Tanigaki K, et al. Notch1 and Notch3 instructively restrict bFGF-responsive multipotent neural progenitor cells to an astroglial fate. Neuron. 2001; 29:45–55. [PubMed: 11182080]

Uryu K, et al. Repetitive mild brain trauma accelerates Abeta deposition, lipid peroxidation, and cognitive impairment in a transgenic mouse model of Alzheimer amyloidosis. J Neurosci. 2002; 22:446–454. [PubMed: 11784789]

Uryu K, et al. Multiple proteins implicated in neurodegenerative diseases accumulate in axons after brain trauma in humans. Exp Neurol. 2007; 208:185–192. [PubMed: 17826768]

Velanac V, et al. Bace1 processing of NRG1 type III produces a myelin-inducing signal but is not essential for the stimulation of myelination. Glia. 2012; 60:203–217. [PubMed: 22052506]

Wyss-Coray T, Mucke L. Inflammation in neurodegenerative disease-a double-edged sword. Neuron. 2002; 35:419–432. [PubMed: 12165466]

Highlights

- APP and the APP secretase proteins, Bace1 and PS1, accumulate acutely after SCI in mice.

- This is a functional accumulation which leads to the production of Aβ pep tide at the injury site.

- Inhibiting Aβ production by targeting the APP secretases results in greater impaired functional recovery after SCI.
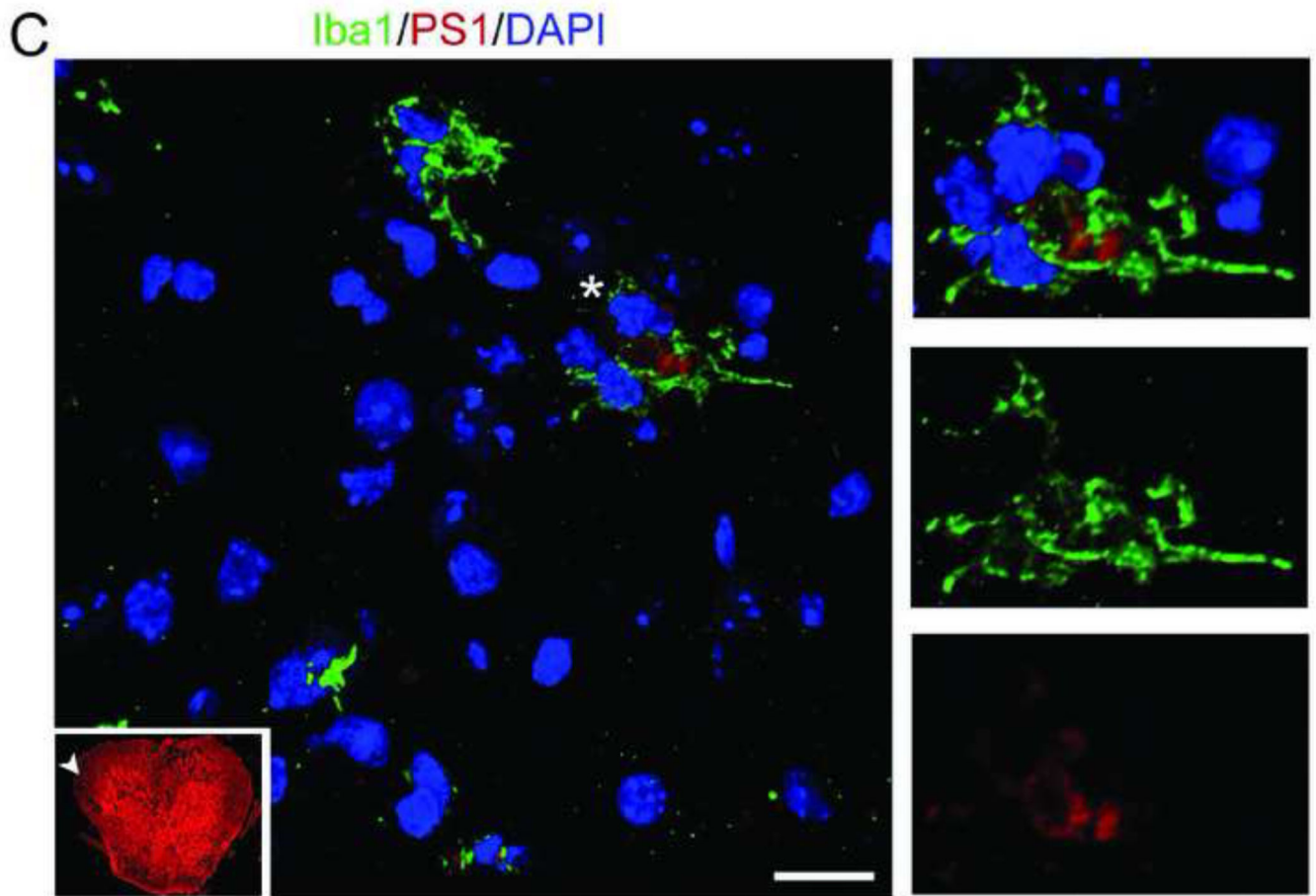
- Aβ may have a beneficial role after SCI.
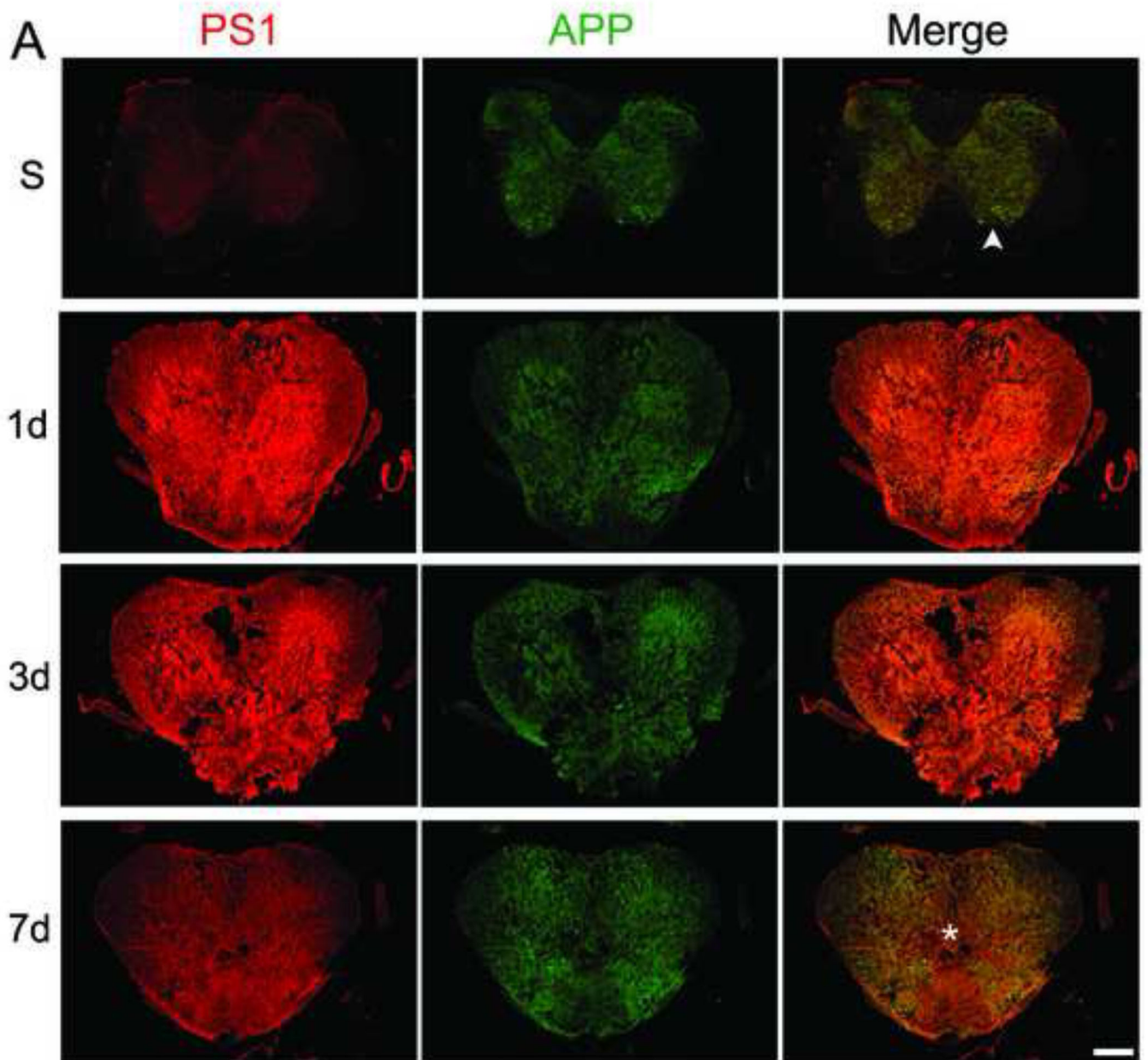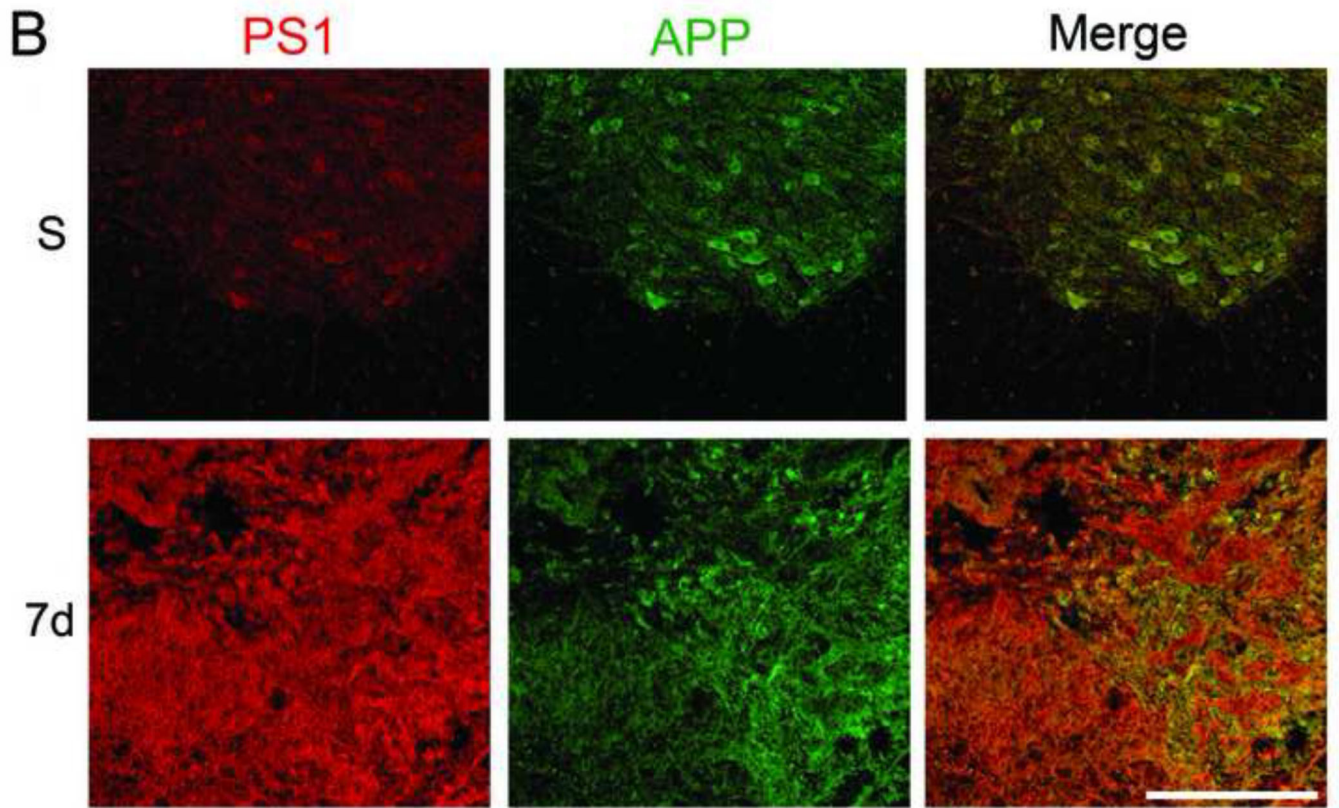
Figure 1. SCI causes an increase in PS1 and APP co-localization
Mice were injured at T9 and sacrificed at 1, 3, and 7 days after contusion injury (n=4/group). The spinal cord sections were stained with APP (green) and PS1 (a component of γ-secretase, red) and confocal tile images were taken with a 20× objective. **A**. Representative images from sham (S, n=4) and 1, 3, and 7 days post-injury (DPI). PS1 and APP are both up-regulated after injury. **B**. The areas identified with arrowhead (in sham) and asterisk (injured, 7 days) in A are magnified to show the co-localization of APP and PS1 before and after injury, as evident by the increase in the overlap of red and green in the merged images at 7 days (Mag. Bar = 500 μm). **C**. Spinal cord sections from 1 DPI were stained with Ibal (green) and PS1 (red). The arrowhead in the 10× thumbnail image indicates the area from which the 63× confocal image was taken. The area identified by asterisk in the 63× was then digitally magnified (Mag. Bar =10 μm).
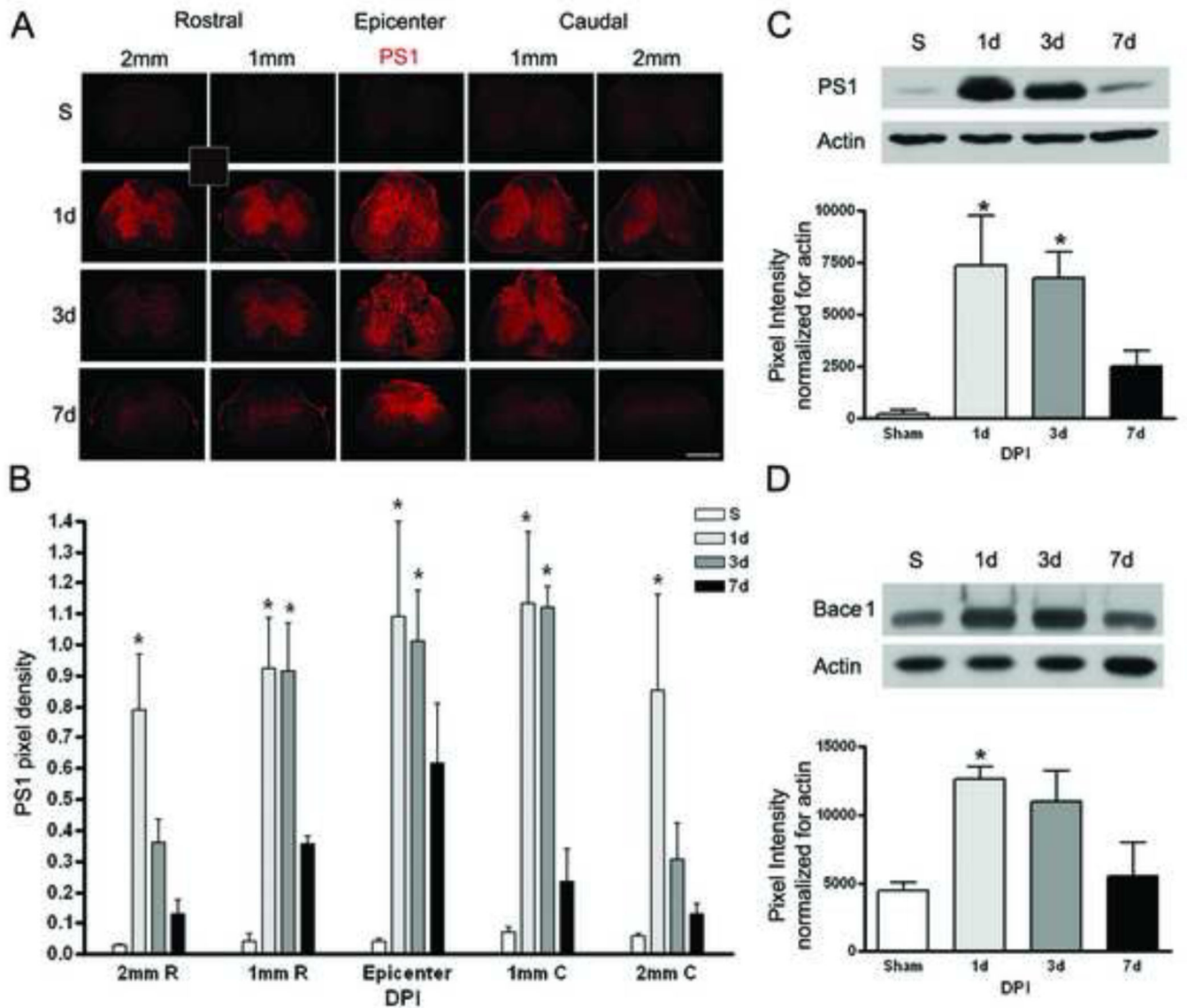
Figure 2. SCI causes an increase in PS1 and Bace1

Mice were injured at T9 and sacrificed at 1, 3, and 7 days post-injury (DPI). Samples were processed for immunofluorescence staining or Western blot analysis. **A**. Representative images from sham (S) and 1, 3, and 7 DPI. PS1, a component of γ-secretase, is increased in the epicenter as well as the sections rostral and caudal to the injury site (Mag. Bar = 500 μm). The thumbnail image shows the no primary antibody negative control. **B**. The quantitation of immuno fluorescence data using image J (n=3), shows a significant increase in PS1 at 1 and 3 DPI as compared to sham in all areas evaluated. **C**. Western blot data confirms the increase of PS1 after SCI (n=3). **D**. Western blot data demonstrate that Bace1 is significantly increased at 1 day after injury (n=3).
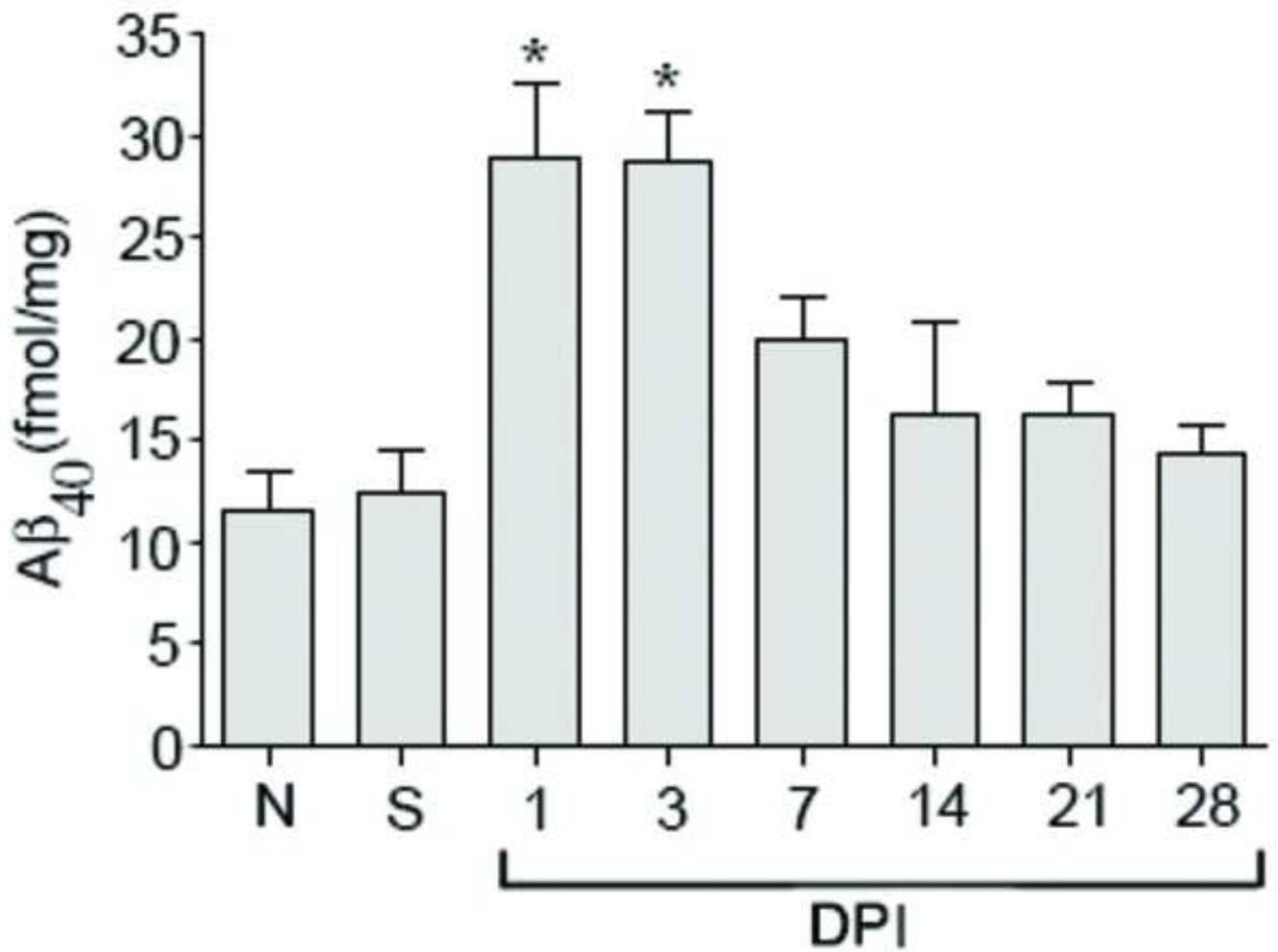
Figure 3. SCI significantly increases Aβ accumulation

$A\beta_{40}$ ELISA was performed in naïve, sham, and at various days (1, 3, 7, 14, 21, and 28) post-injury (n=4/group). Aβ, which is the cleavage product of APP by Bace1 and γ-secretase, is significantly increased at 1 and 3 days after SCI (p value <0.01). There are no differences in the Aβ level between naïve and sham mice.
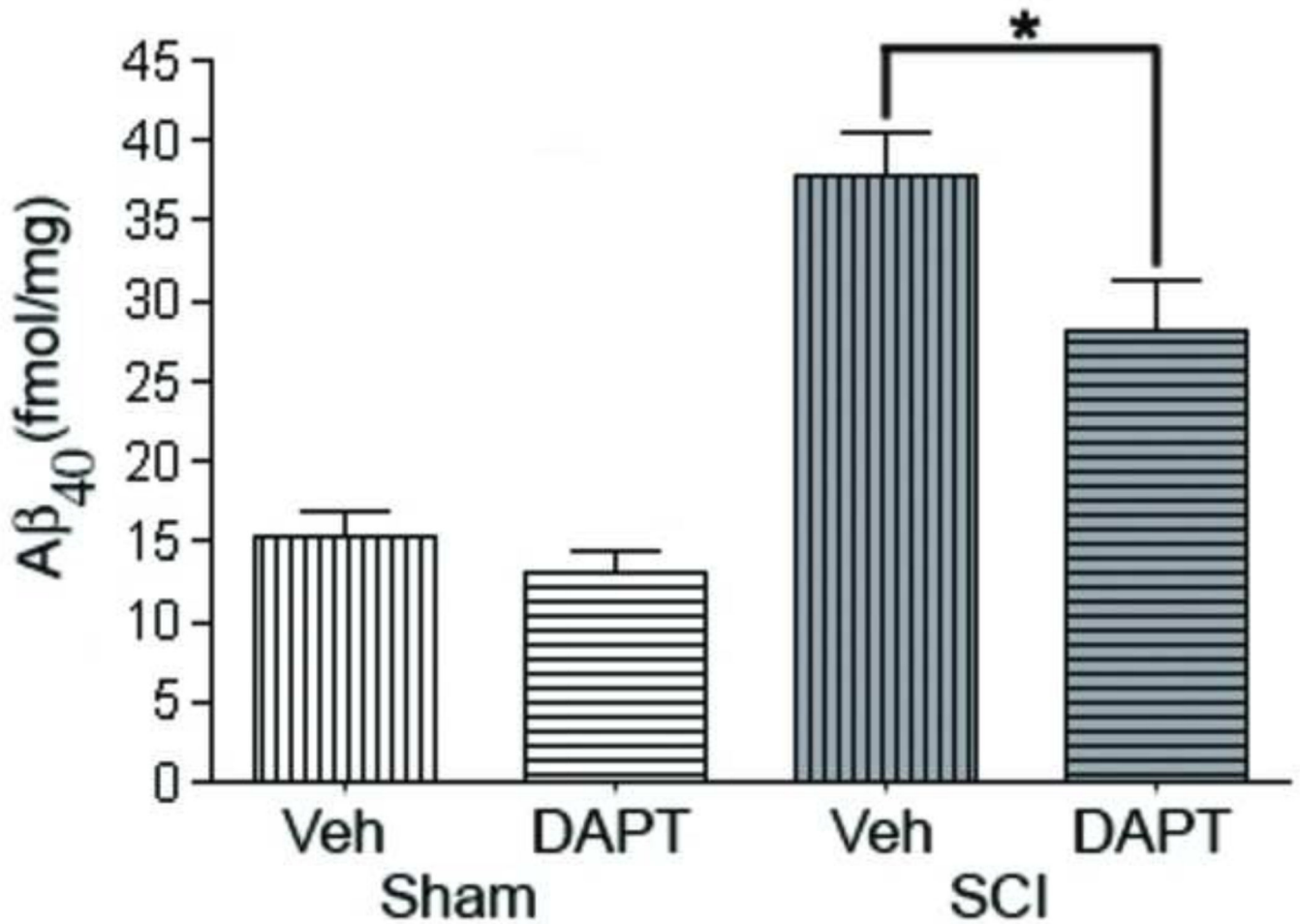
Figure 4. DAPT administration significantly reduces $A\beta_{40}$ after SCI
DAPT (a γ-secretase Inhibitor) and vehicle were administered orally (30mg/kg) twice a day for 3 days to sham and injured mice starting at 15 minutes after injury. Mice were sacrificed (n=4) on the next day after the last dose and $A\beta_{40}$ ELISA was performed. There is no difference between the amount of Aβ present in sham vehicle- and DAPT-treated. However, the DAPT-treated injured mice have significantly (p value < 0.01) less Aβ than the vehicle-treated SCI mice.
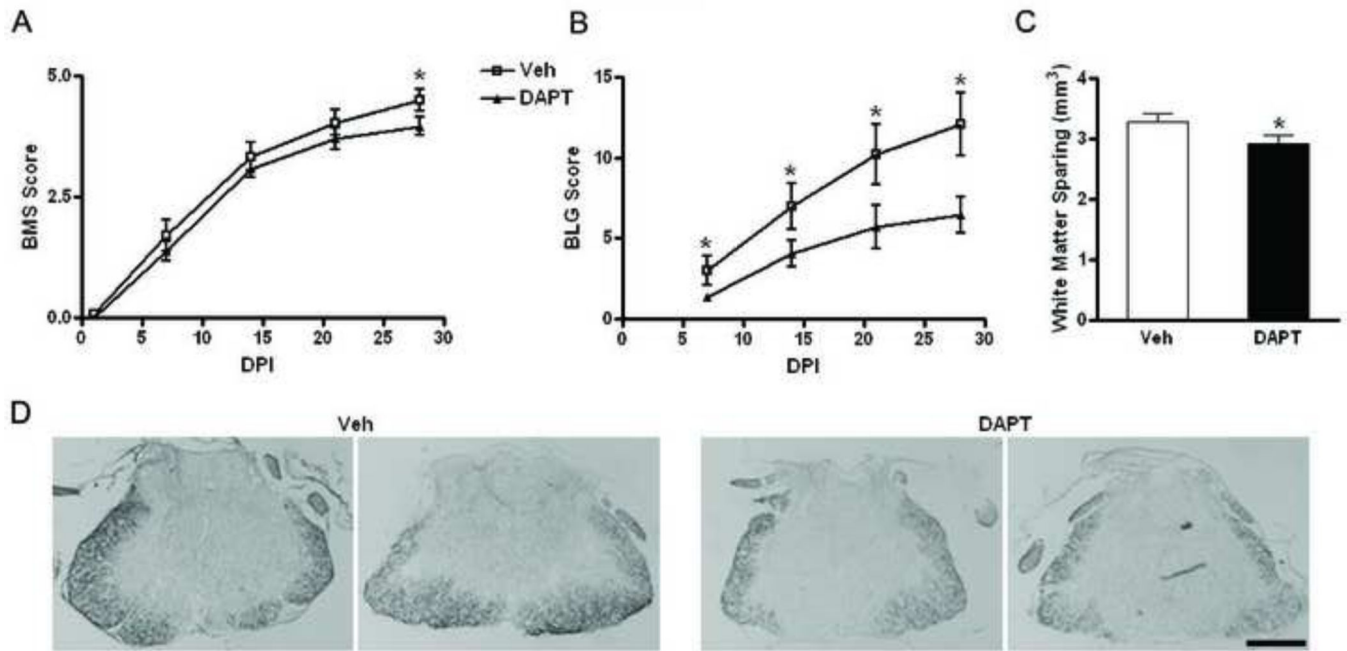
Figure 5. DAPT administration reduces the functional recovery after SCI in mice as measured by behavioral testing

DAPT (30 mg/kg) and vehicle were administered orally twice a day for 10 days (n=12) starting 15 minutes after injury. Mice were evaluated using BMS and BLG scores at 1 day post-injury (DPI) and weekly thereafter. **A**. Vehicle-treated (Veh) mice have a significant (p value < 0.04) higher BMS score at 28 DPI. **B**. The mice were also evaluated based on their stepping using the BLG score. A significant improved performance of vehicle-treated mice is observed as early as 7 DPI. **C**. Sections from spinal cord (n=10) were processed for Eriochrome cyanine R staining and analyzed using sterological techniques. The white matter spared in the vehicle-treated is significantly (p value = 0.0384) higher than the DAPT-treated (DAPT) mice. **D**. Representative images show higher staining present in Veh as compared to DAPT mice at the epicenter (Mag. Bar = 500 μm).
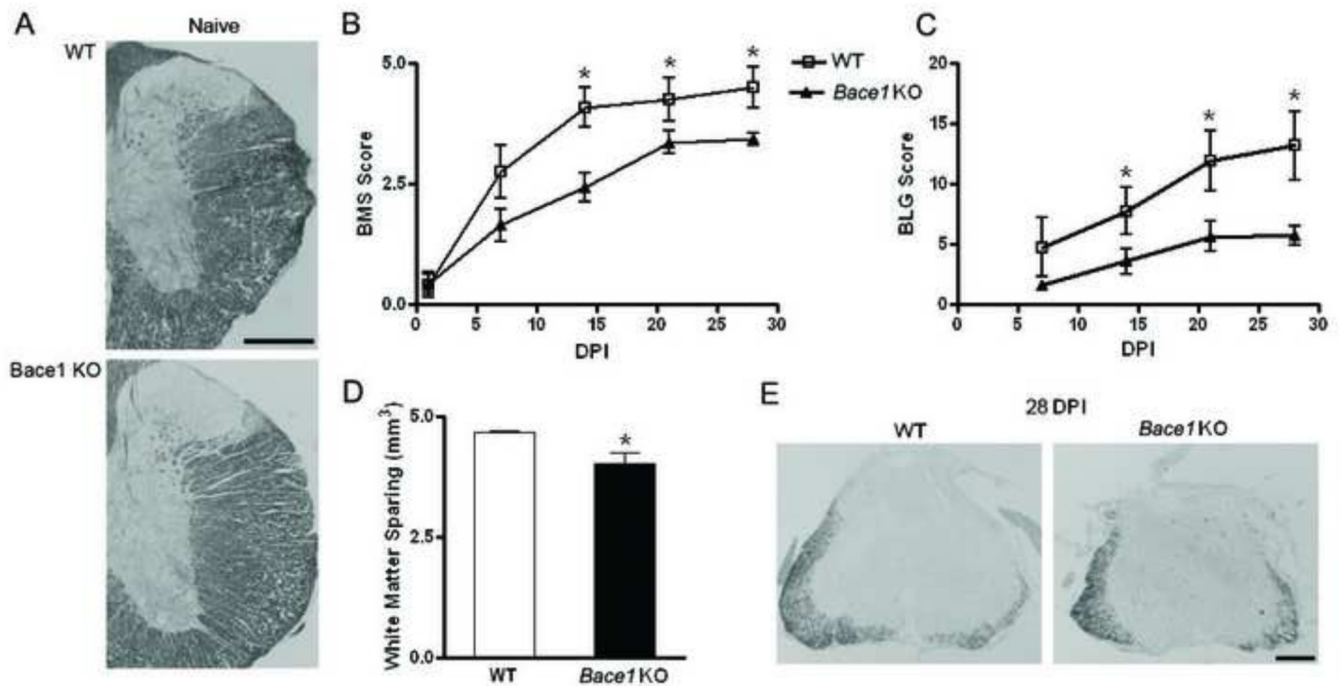
Figure 6. Genetic ablation of Bace1 reduces functional recovery after SCI in mice as measured by behavioral testing

Wild type (WT, n=6) and *Bace1* knockout (*Bace1* KO, n=7) mice were injured and evaluated using BMS and BLG scores at 1 day post-injury (DPI) and weekly thereafter. **A**. Naïve WT and *Bace1* KO mice sacrificed and sections were stained with Eriochrome cyanine R. **B**. WT mice have significant (p value < 0.01 at 28 days) higher BMS score 14 days after injury as compared to *Bace1* KO mice. C. The mice were also evaluated based on their stepping using the BLG score. A significant (p value < 0.01 at 28 days) improved performance in WT mice is observed as early as 14 DPI. **D**. Sections from spinal cord were processed for Eriochrome cyanine R staining and analyzed using sterological techniques. The white matter spared in the WT mice is significantly (p value = 0.0263) higher than the *Bace1* KO mice. **E**. Representative images show higher staining present in the WT as compared to *Bace1* KO mice at the epicenter (Mag. Bar = 500 μm).
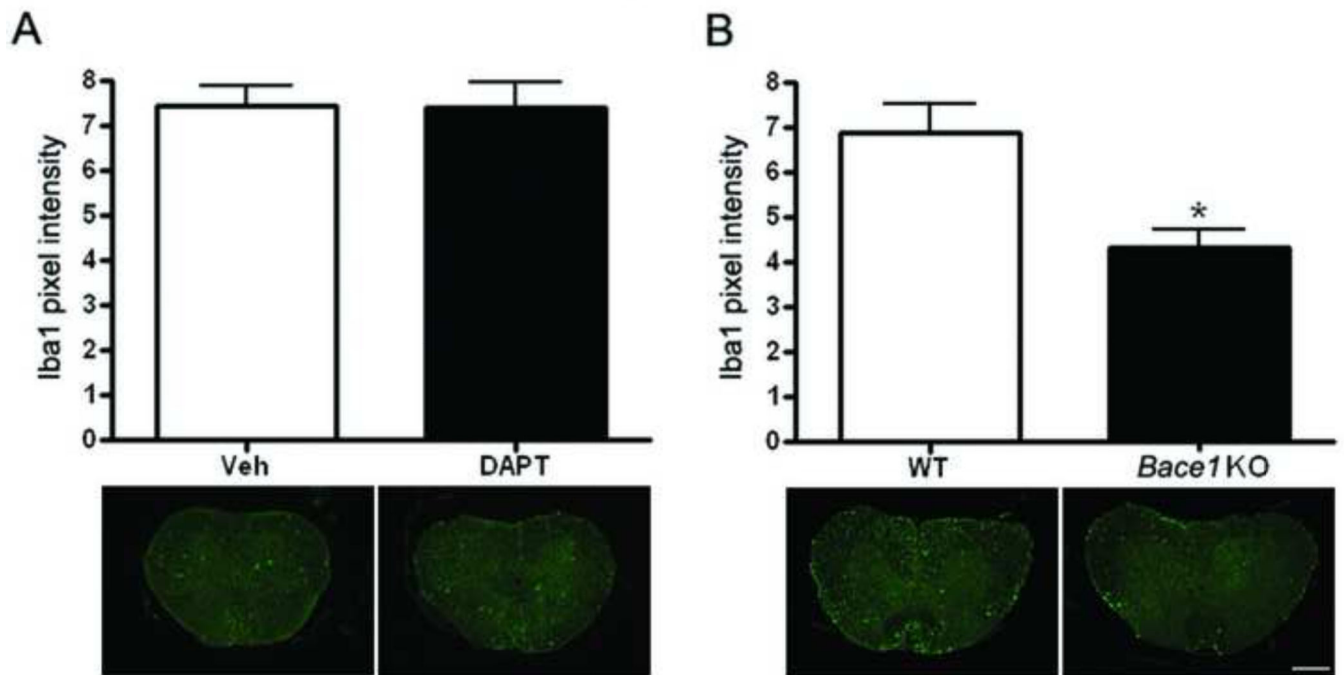
Figure 7. Bace1 KO mice show less microglia after SCI
Sections form vehicle-treated (Veh, n=6), DAPT-treated (DAPT, n=6), Wild type (WT, n=3), and *Bace1* KO (n=3) mice 28 days after injury were stained with Ibal, and staining quantitation was performed using image J. **A**. No differences in microglial number are observed in Veh and DAPT mice as shown in the graph and the representative images. **B**. A significant difference (p value = 0.002) in microglial number is observed between the *Bace1* KO and the WT mice as shown in the graph and the representative images (Mag. Bar = 500 μm).